Journal of Physics: Condensed Matter

Effects of O in a binary-phase TiAl–Ti_3Al alloy: from site occupancy to interfacial energetics

To cite this article: Ye Wei *et al* 2011 *J. Phys.: Condens. Matter* **23** 225504

J. Phys.: Condens. Matter **23** (2011) 225504 (7pp) doi:10.1088/0953-8984/23/22/225504

Effects of O in a binary-phase TiAl–Ti_3Al alloy: from site occupancy to interfacial energetics

Ye Wei[1], Hong-Bo Zhou[2], Ying Zhang[2], Guang-Hong Lu[2] and Huibin Xu[1]

[1] School of Materials Science and Engineering, Beihang University, Beijing 100191, People's Republic of China
[2] Department of Physics, Beihang University, Beijing 100191, People's Republic of China

E-mail: LGH@buaa.edu.cn

Received 20 December 2010, in final form 24 March 2011
Published 17 May 2011
Online at stacks.iop.org/JPhysCM/23/225504

Abstract

We have investigated site occupancy and interfacial energetics of a TiAl–Ti_3Al binary-phase system with O using a first-principles method. Oxygen is shown to energetically occupy the Ti-rich octahedral interstitial site, because O prefers to bond with Ti rather than Al. The occupancy tendency of O in TiAl alloy from high to low is α_2-Ti_3Al to the γ-α_2 interface and γ-TiAl. We demonstrate that O can largely affect the mechanical properties of the TiAl–Ti_3Al system. Oxygen at the TiAl–Ti_3Al interface reduces both the cleavage energy and the interface energy, and thus weakens the interface strength but strongly stabilizes the TiAl/Ti_3Al interface with the O_2 molecule as a reference. Consequently, the mechanical property variation of TiAl alloy due to the presence of O not only depends on the number of TiAl/Ti_3Al interfaces but also is related to the O concentration in the alloy.

(Some figures in this article are in colour only in the electronic version)

1. Introduction

TiAl alloys are considered to be excellent candidates for aerospace applications due to their high melting temperature, low density, high Young's modulus, and good oxidation and creep resistance. However, they suffer from a rather low ductility and toughness at room temperature, which limits their applications [1]. The current emphasis of research is on improving ductility and toughness at room temperature of TiAl alloys while maintaining its attractive high temperature characteristics. Extensive studies of γ-TiAl have been made since the 1980s, particularly on the intrinsic electronic structure, interatomic bonding, grain boundary, impurity, and alloying elements, as well as their effects on mechanical properties [2–14]. As a second phase of the γ-TiAl based alloys, the addition of α_2-Ti_3Al is capable of improving the ductility of TiAl [15]. The interest in Ti–Al based alloys (i.e. in the binary-phase γ/α_2 alloys) is further encouraged because of their superior specific strength and oxidation resistance [16, 17].

It is generally accepted that a trace amount (parts per million, ppm) of impurity would result in an obvious variation of mechanical properties of materials [18–22]. For the TiAl based alloys, O impurity has been paid special attention as it significantly reduces the ductility of TiAl [23]. Oxygen can be absorbed easily from the air during heat-treatments and melting. Liu *et al* [24] studied the competition in occupation between O and H, and revealed that O has a crucial effect on the environmental embrittlement. The O abatement will increase the ductility and change the deformation mechanism [23, 25]. Interstitial O concentration can be lowered by an addition of Er to form an oxide [26]. Oxygen embrittlement has been determined at an electronic level for the defect and bulk TiAl [27, 4]. Dang *et al* investigated the effect of O on the electronic structure, and found that the localized effect of O is not beneficial to the ductility of γ-TiAl [28].

Despite these studies, little work focuses on the effects of impurities on the TiAl/Ti_3Al interface, which is extremely important for the mechanical properties of the binary-phase TiAl–Ti_3Al alloy. In this paper, we investigate the site

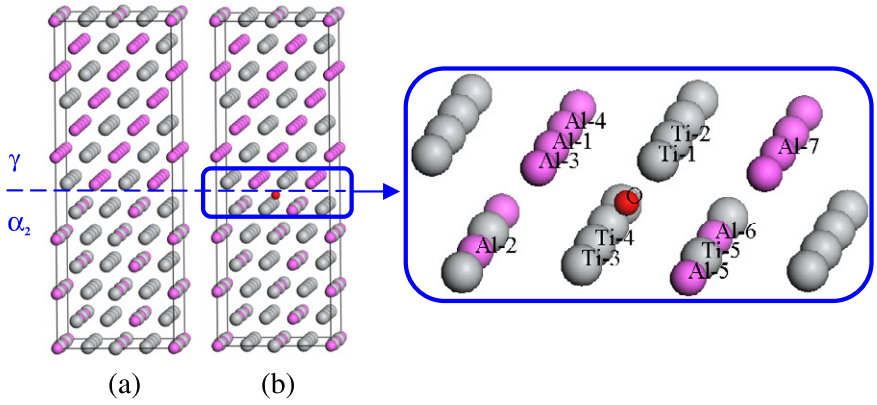

Figure 1. The supercell of the TiAl[1$\bar{1}$0](111) ∥ Ti_3Al[11$\bar{2}$0](0001) interface. (a) The clean system; (b) the system with O at the most stable interstitial site in the interface. Oxygen and its first and second nearest neighbor Al and Ti are labeled. The larger (gray), middle-sized (pink), and smaller (red) spheres represent the Ti, Al, and O atoms, respectively.

preference and energetics of the TiAl/Ti_3Al interface without and with O impurity using a first-principles method. The results are of close relevance to the tailoring of the mechanical properties of TiAl alloys with O impurity.

2. Computational method

We employ a first-principles method based on density functional theory using the Vienna *ab initio* Simulation Package (VASP) [29, 30]. The ion–electron interaction is described by the ultrasoft pseudopotential [31], and the exchange–correlation function is defined by the generalized gradient approximation according to the parameterization of Perdew and Wang [32]. The plane-wave cutoff energy is 350 eV. The relaxation is continued until the forces on all the atoms have converged to less than 10^{-3} eV $Å^{-1}$.

It is known that the binary-phase alloys possess improved ductility and toughness over single phase alloys. The γ-TiAl exhibits the $L1_0$crystal structure and the lattice parameters are calculated to be $a = 3.99$ Å and $c = 4.08$ Å while the α_2-Ti_3Al exhibits the $D0_{19}$ crystalline structure and the lattice parameters are calculated to be $a = 5.74$ Å and $c = 4.65$ Å [33, 34]. The calculated lattice parameters agree well with the corresponding experimental data (for TiAl, $a = 4.00$ Å and $c = 4.08$ Å; for Ti_3Al, $a = 5.77$ Å and $c = 4.62$ Å) [35]. The crystallographic habit plane relationship at the interface is TiAl[1$\bar{1}$0](111) ∥ Ti_3Al[11$\bar{2}$0](0001) (i.e. the close-packed directions are aligned). Such a coherent TiAl/Ti_3Al interface is the only one that has been confirmed by the transmission electron microscopy (TEM) observations experimentally [36–38]. The γ-TiAl has an in-plane lattice spacing of $a_{\langle 110\rangle\{111\}} = 2.83$ Å, which matches well with the α_2-Ti_3Al with an in-plane lattice spacing of $a_{\langle 1000\rangle\langle 0001\rangle} = 2.87$ Å. The layer distance along the [111] direction in TiAl and that along the [0001] direction in Ti_3Al have the same value of $d_{[111]} = d_{[0001]} = 2.32$ Å. These values are derived from the theoretical lattice parameter values. Since the difference of the in-plane lattice spacing between TiAl and Ti_3Al is very small (differs by 1%), the in-plane lattice spacing is assumed to be identical to that of TiAl and then full relaxations are performed. After the relaxation, the lattice parameter of the TiAl–Ti_3Al supercell is 9.89 Å and 11.42 Å, respectively, just between that of TiAl and Ti_3Al, as shown in table 1. The resulting TiAl bulk is tensile while the Ti_3Al bulk is compressed after the interface relaxation. The variation is lower than 2%. This is also the case if we use the lattice parameters of $a_{\langle 110\rangle\{111\}}$ for the TiAl bulk and $a_{\langle 1000\rangle\langle 0001\rangle}$ for the Ti_3Al bulk layers (see table 1). We can thus predict that the bond length variation in the resulting bulk (far from the interface) will also be within 2%.

Table 1. The lattice parameters of the bulk TiAl, Ti_3Al and the TiAl–Ti_3Al system (in units of Å). The variations in percentage between the bulk TiAl(Ti_3Al) and the TiAl–Ti_3Al system are also listed.

	Bulk			Variation (%)	
Lattice parameter	TiAl	Ti_3Al	TiAl–Ti_3Al	TiAl	Ti_3Al
a	9.91	9.94	9.89	−0.2	−0.5
b	11.27	11.46	11.42	1.3	−0.3
$a_{\langle 110\rangle\{111\}}/a_{\langle 1000\rangle\langle 0001\rangle}$	2.83	2.87	2.86	1.1	−0.3

For the TiAl/Ti_3Al interface, the supercell of six layers of TiAl and six layers of Ti_3Al is used, containing 192 atoms, and a 3 × 3 × 1 k-point mesh is used, which is illustrated in figure 1(a). In this structure, the atomic rows composed of Ti atoms only (in both TiAl and Ti_3Al) are aligned continuously across the interface, according to the high-resolution electron microscopy observation [36]. There are two TiAl/Ti_3Al interfaces with the same structure in the supercell. A distance of ∼13.8 Å between these two neighboring interfaces is found to be sufficient to achieve reasonable convergence.

3. Results and discussion

3.1. The site preference of O in the TiAl–Ti_3Al binary-phase alloy

In order to study the effect of O impurity on the structure and bonding properties of binary-phase TiAl–Ti_3Al alloy, it is necessary to identify the site preference of O. Only interstitial sites are considered here due to the smaller atomic radius of O

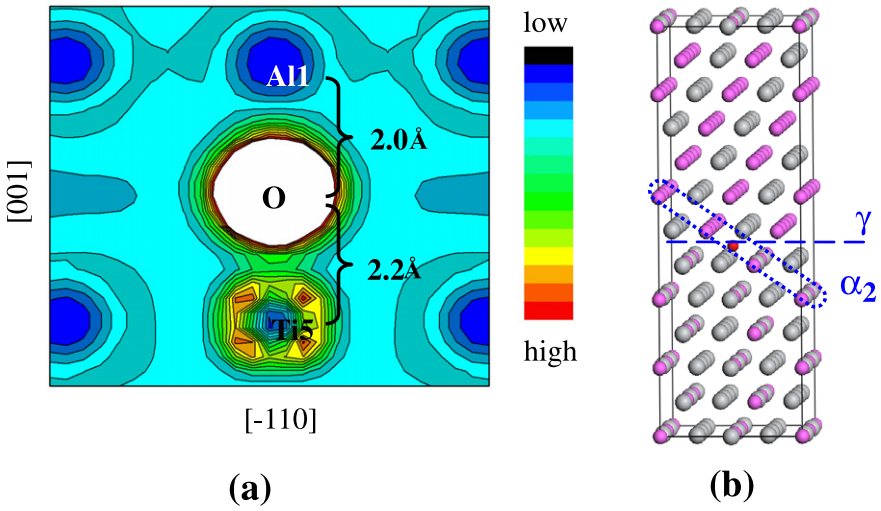

Figure 2. (a) Map of the electronic charge density in the (110) plane of the O-doped binary-phase system. (b) The (110) plane goes across the $TiAl/Ti_3Al$ interface, at which the O atom is included.

in comparison with Ti and Al. We take into account different types of tetrahedral interstitial sites (TIS) and octahedral interstitial sites (OIS).

The formation energy of O (E_O^f) occupying an interstitial site can be calculated by

$$E_O^f = E^T_{TiAl-Ti_3Al-O} - E^T_{TiAl-Ti_3Al} - E_O, \qquad (1)$$

where $E^T_{TiAl-Ti_3Al-O}$ and $E^T_{TiAl-Ti_3Al}$ are the total energies of the $TiAl$–Ti_3Al supercell with and without O, respectively, and E_O is the energy of half of the O_2 molecule, which is −4.35 eV according to the present calculation.

The results are shown in table 2. The negative value of O formation energy indicates that the doped system is more stable than the pure one. This conclusion was reached at static conditions (temperature will destabilize the reaction). Oxygen is shown to be energetically favorable to occupy the Ti-rich OIS surrounded by six Ti atoms in the Ti_3Al phase with the lowest formation energy of −6.23 eV. The occupancy tendency from high to low is α_2-Ti_3Al to the γ-α_2 interface and γ-TiAl, with the corresponding formation energies −6.23 eV, −5.42 eV, and −4.40 eV, respectively. This is consistent with experimental observations [15]. Our results suggest O is preferable to bond with Ti rather than Al. This should be because the electronegativity difference between O (3.44, Pauling electronegativity) and Ti (1.54) is larger than that between O and Al (1.61). This is further confirmed by the electronic structure of the binary-phase system with an O atom at the most stable interstitial site at the $TiAl/Ti_3Al$ interface, as shown in figure 2. Noticeable pair-wise covalent and directional bonding is found in the region between O and its first nearest neighbor (FNN) Ti atom, but no such strong bonding appears between O and Al, indicating that the Ti–O bonding is stronger than the Al–O one.

Now we investigate how the temperature affects the O dissolution by estimating the chemical potential of O_2. The chemical potential of O_2 as a function of temperature (T) and partial pressure of O_2 (P) can be calculated by

$$\mu_O(T, P) = \frac{1}{2}E_{O_2} + \mu_O(T, P^0) + \frac{1}{2}k_B T \ln\left(\frac{P}{P^0}\right), \qquad (2)$$

where E_{O_2} is the total energy of an isolated O_2 molecule, and $\mu_O(T, P^0)$ is the chemical potential of O_2 at temperature T and one standard pressure P^0, which could be obtained from experimental data [39]. For $P = P^0$, the temperature dependence of the chemical potential of O_2 is listed in table 3.

As shown in table 2, the O formation energy in the $TiAl$–Ti_3Al system at absolute 0 K is in the range between −3.20 and −6.23 eV, with half of the energy of the O_2 molecule as the reference (−4.35 eV). Table 3 shows that the chemical potential of O_2 decreases with increasing temperature. Consequently, the formation energy of O increases and thus the stability of the O-doped binary system decreases with increasing temperature, but the occupancy preference remains unchanged. Further, the formation energy of O remains negative until very high temperatures (as high as

Table 2. Formation energies (in eV) of the O atom at different types of TIS and OIS in the binary-phase $TiAl$–Ti_3Al supercell. ΔE is the energy increment from the most stable system; in brackets is the atom species and the number surrounding O.

Structure		Formation energy (eV)	ΔE (eV)
Ti_3Al	Ti-OIS (6Ti)	−6.23	0
	OIS (4Ti–2Al)	−4.75	1.48
	TIS (3Ti–1Al)	−4.20	2.03
	TIS (3Ti–1Al)	−3.83	2.40
$TiAl/Ti_3Al$ interface	Ti-OIS (5Ti–1Al)	−5.42	0.81
	OIS (3Ti–3Al)	−4.09	2.14
	OIS (4Ti–2Al)	−4.69	1.54
	TIS (3Ti–1Al)	−4.23	2.00
	TIS (2Ti–2Al)	−3.45	2.78
TiAl	TIS (2Ti–2Al)	−3.49	2.74
	OIS (2Ti–4Al)	−3.20	3.03
	Ti-OIS (4Ti–2Al)	−4.40	1.83

Table 3. Chemical potential of O_2 at different temperatures.

T (K)	0	500	1000	2000	2500	3000	4000	4500	5000
μ_O (eV)	−4.35	−4.89	−5.5	−6.83	−7.54	−8.27	−9.78	−10.55	−11.34

Table 4. Cleavage energies (γ_{cl}) of the TiAl(111), Ti_3Al(0001), and TiAl–Ti_3Al interface for both the clean and O-doped systems. $\Delta\gamma_{cl}$ is the energy variation with reference to the respective clean system.

	γ_{cl} (J m^{-2})	$\Delta\gamma_{cl}$ (%)
TiAl–Ti_3Al	3.62	0
TiAl–Ti_3Al–1O	3.47	−4
TiAl–Ti_3Al–2O	3.33	−8
TiAl(111)	3.45	0
TiAl(111)–O	3.23	−6
TiAl(111)–2O	3.00	−13
Ti_3Al(0001)	4.03	0
Ti_3Al(0001)–O	3.99	−1
Ti_3Al(0001)–2O	3.94	−2

Table 5. The bond lengths of the Al–Ti, Ti–Ti, and Al–Al among first and second nearest neighbor atoms of O's interstitial site, crossing the TiAl/Ti_3Al interface for the clean system and the O-doped system, and the increments of bond lengths caused by O (in units of Å).

	Clean system	O-doped system	Increment
Ti1–Ti3/Ti2–Ti4	2.826	2.985	0.159
Al1–Ti3/Al1–Ti4	2.837	2.955	0.118
Ti1–Ti5/Ti2–Ti5	2.896	2.975	0.079
Al1–Al2	2.851	2.882	0.031
Ti3–Al3/Ti4–Al4	2.843	2.873	0.030
Ti1–Al5/Ti2–Al6	2.844	2.867	0.023
Ti5–Al7	2.946	2.968	0.022

2500 K). Hence, basically O can still stabilize the TiAl–Ti_3Al system.

3.2. Effects of O on the cleavage energy of the TiAl/Ti_3Al interface

We now turn to investigate the bonding property of the interface in binary-phase TiAl–Ti_3Al alloy. We calculated the cleavage energy of the TiAl/Ti_3Al interface with and without an O atom occupying the energetically preferred Ti-OIS (5Ti–1Al) in the TiAl/Ti_3Al interface. We use the Ti_3Al–O system as a reference system (i.e. O situated at the surface of Ti_3Al after the cleavage) because the present results indicate that energetically O tends to stay in Ti_3Al rather than TiAl (table 2). In order to investigate the effect of O concentration, the two-O-atom case at the interface is also taken into account. Both O atoms are placed in the energetically preferred Ti-OIS (5Ti–1Al) and the distance between them is 5.7 Å. Such a configuration is found to be energetically stable by our calculation.

The cleavage energy γ_{cl} is defined as the energy required per unit area to separate the solid into two semi-infinite halves by creating two surfaces, neglecting diffusional and plastic degrees of freedom. The cleavage energy can be a direct measure of the interface bond strength, considered as the lower bound to the actual energy cost measured in a cleavage experiment [40]. Here, the cleavage energies (γ_{cl}) of the TiAl/Ti_3Al interface without and with O are then calculated through

$$\gamma_{cl(TiAl-Ti_3Al)} = \frac{E^{slab}_{TiAl} + E^{slab}_{Ti_3Al} - E_{TiAl-Ti_3Al}}{2A} \quad (3)$$

and

$$\gamma_{cl(TiAl-Ti_3Al-O)} = \frac{E^{slab}_{TiAl} + E^{slab}_{Ti_3Al-O} - E_{TiAl-Ti_3Al-O}}{2A}, \quad (4)$$

where $E_{TiAl-Ti_3Al}$ and $E_{TiAl-Ti_3Al-O}$ are the total energy of the clean and O-doped binary-phase system, A is the interface area of the binary-phase system, and E^{slab}_{TiAl} and $E^{slab}_{Ti_3Al}$ are the total energies of the six-layer TiAl and Ti_3Al with the same-size supercells as the binary-phase system, but removing the Ti_3Al and TiAl layers, respectively. $E^{slab}_{Ti_3Al-O}$ is the total energy of the six-layer Ti_3Al with O at the most stable site at both surfaces in the supercell. For the calculation of the energy of the separate TiAl and Ti_3Al phases, the slabs have been optimized.

In addition, we calculated the cleavage energy of TiAl(111) and Ti_3Al(0001) with and without O. The order of the bond strength is $Ti_3Al(0001)$ > TiAl/Ti_3Al interface > TiAl(111), and the corresponding order of cleavage energy is 4.03 > 3.62 > 3.45 J m^{-2}. The cleavage energy decreases with the introduction of O to all the interface systems, and it further decreases when the amount of O increases. The decrements of cleavage energy in percentages are listed in table 4, suggesting that all three kinds of interfaces in TiAl alloy are weakened by the introduction of O. Particularly, the cleavage energy of the clean TiAl/Ti_3Al interface is 3.62 J m^{-2} and decreases to 3.47 J m^{-2} and 3.33 J m^{-2} after the addition of one O and two O, respectively. Moreover, with the O concentration identical in all the interface systems, the order of bond strength remains the same as that of the clean systems. Despite the lowest cleavage energy of the TiAl(111) in both the clean and O-doped systems, it is difficult to clarify whether fracture occurs in the TiAl, Ti_3Al lamellae, or along the TiAl/Ti_3Al interface, because the local O concentration plays an important role as well.

We now investigate the intrinsic mechanism of the weakening effect of O-doping at the TiAl/Ti_3Al interface. We calculate the bond lengths of the Al–Ti, Ti–Ti, and Al–Al among first and second nearest neighbor atoms of the O interstitial site, crossing the TiAl/Ti_3Al interface with and without O existing. As listed in table 5, the bond lengths are increased due to O-doping, and the increment of the bond length of the first nearest neighbor atoms is larger than that of the second nearest neighbor atoms, implying a decrease of bond strength at the TiAl/Ti_3Al interface surrounding O in spite of the newly formed O–Ti/O–Al bonds.

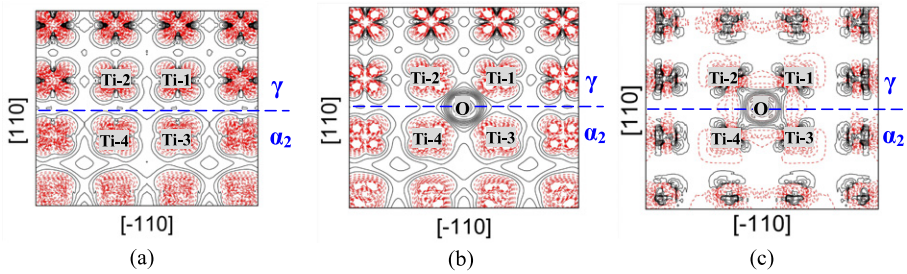

Figure 3. The charge density difference contour maps on the (001) Ti layer cross the TiAl/Ti_3Al interface. (a) and (b) show the first charge density difference contour maps for the clean system and the O-doped system, respectively, while (c) shows the second charge density difference contour map. Black solid and red dotted lines correspond to the gain and the loss of electrons, respectively.

Furthermore, we investigate the spatial redistribution of electron density induced by O impurities. We plotted the first charge density difference contour maps on the (001) Ti layer, crossing the TiAl/Ti_3Al interface, of the clean and the O-doped systems in figures 3(a) and (b), which are obtained by subtracting the electron density of free atoms from that of the binary-phase system. We also plotted the second charge density difference contour map on the (001) Ti layer in figure 3(c), by subtracting the first electron density difference of the clean system from that of the O-doped binary-phase system. We can clearly see the O-induced charge redistribution from the charge density difference maps. In figures 3(a) and (b), directional charge redistribution is found between Ti atoms in the TiAl phase (the upper part of figure 3), indicating an obvious Ti_d–Ti_d directional bonding. In figure 3(b), the charge accumulates in the region between O and its FNN Ti atoms, indicating a strong Ti–O bonding. In figure 3(c), we can clearly see the charge density reduction among the FNN Ti sites and the charge density increment between O and its FNN Ti atoms, implying that the charge transfers from the region between Ti–Ti to O–Ti and the Ti_d–Ti_d bonding is weakened. It could be deduced that the forming of O–Ti bonding is not strong enough to compensate for the decrease of the Ti–Ti and Ti–Al bonding, and the overall effect of O-doping is the decrease of the interface bond strength.

3.3. Effects of O on the TiAl/Ti_3Al interface energy

Now we investigate the effects of O on the interface energy of the TiAl/Ti_3Al system, which can be viewed as the energy required to form the interface from bulk materials. In contrast to the cleavage energy, it is not an absolute measure of the interface bond strength; instead, it compares the interfacial bonds to the bonding in the bulk material [41]. All the interfacial energies are calculated after atomic relaxations, although the lattice relaxations near the interface are small. Here, the interface energies (γ_{int}) of the TiAl/Ti_3Al interface without and with O are then calculated through

$$\gamma_{\mathrm{int}_{(\mathrm{TiAl-Ti_3Al})}} = \frac{E_{\mathrm{TiAl-Ti_3Al}} - E^{\mathrm{bulk}}_{\mathrm{TiAl}} - E^{\mathrm{bulk}}_{\mathrm{Ti_3Al}}}{2A} \quad (5)$$

and

$$\gamma_{\mathrm{int}_{(\mathrm{TiAl-Ti_3Al-O})}} = \frac{E_{\mathrm{TiAl-Ti_3Al-2O}} - E^{\mathrm{bulk}}_{\mathrm{TiAl}} - E^{\mathrm{bulk}}_{\mathrm{Ti_3Al}} - E^{\mathrm{ref}}_{\mathrm{O_2}}}{2A}, \quad (6)$$

Table 6. The interface energies of the clean TiAl/Ti_3Al interface ($\gamma_{int(TiAl/Ti3Al)}$) and the O-doped TiAl/Ti_3Al interface ($\gamma_{int(TiAl/Ti3Al-O)}$). For the calculation of $\gamma_{int(TiAl/Ti3Al-O)}$, three different reference systems are taken into account.

	meV Å^{-2}	mJ m^{-2}
$\gamma_{int(TiAl/Ti3Al)}$	7	120
$\gamma_{int(TiAl/Ti3Al-O)}$ with different references		
O_2 molecule	−39	−631
O in TiAl	−4	−59
O in Ti_3Al	14	222

where $E_{\mathrm{TiAl-Ti_3Al}}$ and $E_{\mathrm{TiAl-Ti_3Al-2O}}$ are the total energies of the clean and the O-doped binary-phase systems. A is the interface area, $E^{\mathrm{bulk}}_{\mathrm{TiAl}}$ and $E^{\mathrm{bulk}}_{\mathrm{Ti_3Al}}$ are the total energies of the 96-atom TiAl and Ti_3Al, respectively, and $E^{\mathrm{ref}}_{\mathrm{O_2}}$ is the reference energy of the O_2 molecule. During the formation of the interface, O at the interface can be absorbed from the air, or diffused from the TiAl or Ti_3Al phase. The interface energy of the O-doped system depends on the reference system of O. We consider all the possible cases for the O from different reference systems, i.e. the O_2 molecule, TiAl, and Ti_3Al. In equation (6), $E^{\mathrm{ref}}_{\mathrm{O_2}}$ is different depending on the system that O is from.

As listed in table 6, the interface energy is calculated to be 120 mJ m^{-2} for the clean TiAl/Ti_3Al interface. As a comparison, the interface energy of the clean TiAl–Ti_3Al interface was calculated to be 110 mJ m^{-2} by Fu *et al* [42]. While it decreases to −631 mJ m^{-2} and −59 mJ m^{-2} for the TiAl/Ti_3Al–O system with reference to the O_2 molecule and O in TiAl, respectively. The results indicate that O can stabilize the TiAl/Ti_3Al interface in these two cases, and the O_2 molecule case is much more stable. In contrast, the interface energy increases to 222 mJ m^{-2} with reference to O in Ti_3Al, indicating that the stability of the interface is weakened in this case.

The experimental results [43] show that the TiAl–Ti_3Al alloys containing O less than 1000 ppm (weight) do not exhibit fully lamellar microstructures, as was expected by the choice of the heat treatment. For the alloys containing O more than 1000 ppm, the alloys exhibit the fully lamellar microstructure due to the O stabilization. As a matter of fact, almost all the TiAl/Ti_3Al interfaces in the alloys exist in the lamellar microstructure, which suggests the TiAl/Ti_3Al interfaces are

stabilized by the presence of O. Thermodynamically, O is most probably from the O_2 molecule or TiAl rather than Ti_3Al according to the calculated O formation energy (table 2). This could be the reason why O has been observed to stabilize the TiAl/Ti_3Al interfaces experimentally.

Such a positive value of the interface energy suggests that the clean TiAl/Ti_3Al interface is not energetically stable. For the O-doped system, if we choose the O_2 molecule as a reference, the interface energy of the O-doped TiAl/Ti_3Al interface is much lower than the clean case. The interface energy after the addition of O is decreased by as much as ∼6 times, suggesting O will strongly stabilize the TiAl/Ti_3Al interface and make it easier to form, which is consistent with the experimental results [43]. The decrement of interface energy lies in the formation of the O–Ti bonding after the addition of O at the interface.

Experimentally, it is desirable to prepare the TiAl alloys with a suitable heating treatment, making both grains and lamellae of alloys as fine as possible [44–48]. This suggests that the ductility of the TiAl alloys strongly depends on the TiAl/Ti_3Al interface area. Larger TiAl/Ti_3Al interface area should correspond to the higher ductility. According to the present calculation with reference to the O_2 molecule, the presence of O makes the TiAl/Ti_3Al interface easier to form by largely decreasing the interface energy. On the other hand, the experimental results show that the increased O content is well correlated with reduced ductility [23]. The O-induced brittleness of the TiAl alloy might be due to the weakening of the interfaces as well as the pinning of the dislocations by O [49]. Consequently, the mechanical property variation of TiAl alloy due to the presence of O not only depends on the number of TiAl/Ti_3Al interfaces but also is related to the O concentration in the alloy.

4. Summary

In summary, we investigated the effect of O on electronic structure, cleavage energy, and interface energy in a TiAl/Ti_3Al binary-phase system using a first-principles method. Oxygen is shown to energetically occupy the Ti-rich octahedral interstitial site, because O prefers to bond with Ti rather than Al. The occupancy tendency of O in TiAl alloy from high to low is α_2-Ti_3Al to the γ-α_2 interface and γ-TiAl. The cleavage energy of the TiAl/Ti_3Al interface decreases to 3.47 J m^{-2} due to the presence of O, 4% lower than that of the O-free TiAl/Ti_3Al interface, indicating that the TiAl/Ti_3Al interface is weakened with O existing. For the O-doped system, if we choose the O_2 molecule as a reference, O can largely decrease the TiAl/Ti_3Al interface energy, with an implication that O can strongly stabilize the TiAl/Ti_3Al interface and make it easier to form. Consequently, the mechanical property variation of TiAl alloy due to the presence of O not only depends on the number of TiAl/Ti_3Al interfaces but also is related to the O concentration in the alloy.

Acknowledgment

The authors greatly appreciate the helpful discussions with Dr Jia-Xiang Shang at Beihang University.

References

[1] Kim Y W and Froes F H 1990 *High-Temperature Aluminides and Intermetallics* ed S H Whang, C T Liu, D P Pope and J O Stiegler (Warrendale, PA: IMS) p 465
[2] Greenberg B F, Anisimov V I, Gornostirev Y N and Taluts G G 1988 *Scr. Metall.* **22** 859
[3] Morinaga M, Satio J, Yukawa N and Adachi H 1990 *Acta Metall. Mater.* **38** 25
[4] Song Y, Tang S P, Xu J H, Mryasov O N, Freeman A J, Woodard C and Dimiduk D M 1994 *Phil. Magn.* B **70** 987
[5] Simmons J P, Rao S I and Dimiduk D M 1998 *Phil. Magn. Lett.* **77** 327
[6] Mryasov N, Gornostyrev Y N and Freeman A J 1998 *Phys. Rev.* B **58** 11927
[7] Appel F 2001 *Mater. Sci. Eng.* A **317** 115
[8] Zhang W J, Reddy B V and Deevi S C 2001 *Scr. Mater.* **45** 645
[9] Hsiung L, Nieh T, Choi B W and Wadaworth J 2002 *Mater. Sci. Eng.* A **329** 637
[10] Mishin Y and Herzig C 2002 *Acta Mater.* **48** 589
[11] Song Y, Guo Z X and Yang R 2002 *J. Light Met.* **2** 115
[12] Yu R, He L L and Ye H O 2002 *Phys. Rev.* B **65** 184102
[13] Zope R R and Mishin Y 2003 *Phys. Rev.* B **68** 024102
[14] Dang H L, Wang C Y and Yu T 2007 *J. Appl. Phys.* **101** 083702
[15] Menand A, Zapolsky-Tatarenko H and Nérac-Partaix A 1998 *Mater. Sci. Eng.* A **250** 55–64
[16] Kim Y W and Dimiduk D M 1991 *J. Met.* **43** 40
[17] Yamaguchi M and Inui H 1993 *Structural Intermetallics* ed R Darolia, J J Lewandowski, C T Liu, P L Martin, D B Miracle and M V Nathal (Warrendale, PA: TMS) p 127
[18] Zhang Y, Lu G H, Hu X L, Wang T, Kohyama M and Yamamoto R 2007 *J. Phys.: Condens. Matter* **19** 456225
[19] Lu G H, Deng S, Wang T, Kohyama M and Yamamoto R 2004 *Phys. Rev.* B **69** 134106
[20] Lu G H, Zhang Y, Deng S, Wang T, Kohyama M, Yamamoto R, Liu F, Horikawa K and Kanno M 2006 *Phys. Rev.* B **73** 224115
[21] Zhang Y, Lu G H, Deng S, Wang T, Shu X, Kohyama M and Yamamoto R 2006 *J. Phys.: Condens. Matter* **18** 5121
[22] Zhang Y, Lu G H, Deng S, Wang T, Xu H, Kohyama M and Yamamoto R 2007 *Phys. Rev.* B **75** 174101
[23] Kawabata T, Tadano M and Izumi O 1988 *Scr. Metall.* **22** 1725
[24] Liu Y, Chen K Y, Zhang J H, Hu Z Q, Lu G and Kioussis N 1997 *J. Phys.: Condens. Matter* **9** 9829
[25] Huang S C and Hall E L 1991 *Metall. Mater. Trans.* A **22** 427
[26] Vasudevan V K, Court S A, Kurath P and Fraser H L 1989 *Scr. Metall.* **23** 467
[27] Woodward C, MacLaren J M and Rao S 1992 *J. Mater. Res.* **7** 1735
[28] Dang H L, Wang C Y and Yu T 2006 *J. Phys.: Condens. Matter* **18** 8803
[29] Kresse G and Hafner J 1993 *Phys. Rev.* B **47** 558
[30] Kresse G and Furthmüller J 1996 *Phys. Rev.* B **54** 11169
[31] Vanderbilt D 1990 *Phys. Rev.* B **41** 7892
[32] Perdew J P, Chevary J A, Vosko S H, Jackson K A, Pederson M R and Fiolhais C 1992 *Phys. Rev.* B **46** 6671
[33] Zhou H B, Wei Y, Liu Y L, Zhang Y and Lu G-H 2010 *Modelling Simul. Mater. Sci. Eng.* **18** 015007
[34] Wei Y, Zhang Y, Lu G-H and Xu H B 2010 *Int. J. Mod. Phys.* B **24** 2749–55
[35] Pearson W B 1987 *A Handbook of Lattice Spacing and Structure of Metals and Alloys* (Oxford: Pergamon) pp 1–2
[36] Inui H, Nakamura A, Oh M H and Yamaguchi M 1991 *Ultramicroscopy* **39** 268
[37] Fischer F D, Waitz T, Scheu Ch, Cha L, Dehme G, Antretter T and Clemens H 2010 *Intermetallics* **18** 509–17

[38] Koizumi Y, Sugihara A, Tsuchiya H, Minamino Y, Fujimoto S, Yasuda H and Yoshiya M 2010 *Acta Mater.* **58** 2876–86
[39] Stull D R and Prophet H 1971 *JANAF Thermochemical Tables* 2nd edn (Washington, DC: US National Bureau of Standards)
[40] Gong H R 2009 *Intermetallics* **17** 562–7
[41] Christensen M, Dudiy S and Wahnström G 2002 *Phys. Rev.* B **65** 045408
[42] Fu C L 1997 *Scr. Mater.* **37** 1453–9
[43] Lamirand M, Bonnentien J L, Ferrière G, Guérin S and Chevalier J P 2007 *Scr. Mater.* **6** 325–8
[44] Chan K S and Kim Y W 1995 *Acta Metall. Mater.* **43** 439–51
[45] Umakoshi Y, Nakano T, Takenaka T, Sumimoto K and Yamane T 1993 *Acta Metall. Mater.* **41** 1149
[46] Umeda H, Kishida K, Inui H and Yamaguchi M 1997 *Mater. Sci. Eng.* A **239–240** 336
[47] Maruyama K, Yamada N and Sato H 2001 *Mater. Sci. Eng.* A **319–321** 360
[48] Maruyama K, Suzuki G, Kim H Y, Suzuki M and Sato H 2002 *Mater. Sci. Eng.* A **329–331** 190
[49] Morris M A 1996 *Intermetallics* **4** 417–26